The impact of spring subsurface soil temperature anomaly in the western U.S. on North American summer precipitation: A case study using regional climate model downscaling

Yongkang Xue,[1,2] Ratko Vasic,[3] Zavisa Janjic,[3] Y. M. Liu,[4] and Peter C. Chu[5]

Received 27 February 2012; revised 24 April 2012; accepted 25 April 2012; published 2 June 2012.

[1] This study explores the impact of spring subsurface soil temperature (SUBT) anomaly in the western U.S. on North American summer precipitation, mainly southeastern U.S., and possible mechanisms using a regional climate Eta model and a general circulation model (GCM). The GCM produces the lateral boundary condition (LBC) for the Eta model. Two initial SUBT conditions (one cold and another warm) on May 1st were assigned for the GCM runs and the corresponding Eta runs. The results suggest that antecedent May 1st warm initial SUBT in the western U.S. contributes positive June precipitation over the southern U.S. and less precipitation to the north, consistent with the observed anomalies between a year with a warm spring and a year with a cold spring in the western U.S. The anomalous cyclone induced by the surface heating due to SUBT anomaly propagated eastward through Rossby waves in westerly mean flow. In addition, the steering flow also contributed to the dissipation of perturbation in the northeastern U.S. and its enhancement in southeastern U.S. However, these results were obtained only when the Eta model run was driven by the corresponding GCM run. When the same reanalysis data were applied for both (cold and warm initial SUBT) Eta runs' LBCs, the precipitation anomalies could not be properly produced, indicating the intimate dependence of the regional climate sensitivity downscaling on the imposed global climate forcing, especially when the impact was through wave propagation in the large-scale atmospheric flow.

Citation: Xue, Y., R. Vasic, Z. Janjic, Y. M. Liu, and P. C. Chu (2012), The impact of spring subsurface soil temperature anomaly in the western U.S. on North American summer precipitation: A case study using regional climate model downscaling, *J. Geophys. Res.*, *117*, D11103, doi:10.1029/2012JD017692.

1. Introduction

[2] Modeling studies and data analyses based on ground and satellite data have demonstrated that the land surface state variables, such as soil moisture, snow, vegetation, and soil temperature, interact with the atmosphere [e.g., *Cayan*, 1996; *Zhou et al.*, 2003; *Mahanama et al.*, 2008; *Dirmeyer et al.*, 2009]. However, the memory inherent in the land surface state and mechanisms through which it interacts with atmospheric states and circulation are still not well understood. Thus far, most modeling studies have focused on soil moisture and snow with less attention given to soil temperature. In contrast, the effect of sea surface temperature (SST) has been extensively investigated due to ocean water's large heat capacity (roughly three times more compared with soil) and significant heat horizontal transport.

[3] Recently, a few studies have explored subsurface soil temperature's (SUBT) role in the climate system. SUBT represents soil energy status and heat storage, as well as heat transfer conditions. *Mahanama et al.* [2008] conducted two experiments with a general circulation model (GCM) with specified SUBT and interactive SUBT, which were calculated using a variant of the Force-Restore Method [*Deardorff*, 1978]. They interpreted the difference between these two experiments as the impact of SUBT. The study revealed that allowing an interactive SUBT did significantly increase surface air temperature variability and memory in most regions. In many regions, however, the impact was negligible, particularly during boreal summer. Meanwhile, their study also revealed some evidence of a connection between the late spring temperature

[1]Department of Geography, University of California, Los Angeles, California, USA.
[2]Department of Atmospheric and Oceanic Sciences, University of California, Los Angeles, California, USA.
[3]National Center for Environmental Prediction, NOAA, Camp Springs, Maryland, USA.
[4]State Key Laboratory of Numerical Modeling for Atmospheric Sciences and Geophysical Fluid Dynamics, Institute of Atmospheric Physics, Chinese Academy of Sciences, Beijing, China.
[5]Naval Ocean Analysis and Prediction Laboratory, Department of Oceanography, Naval Postgraduate School, Monterey, California, USA.

Corresponding author: Y. Xue, Department of Geography, University of California, Los Angeles, 1255 Bunche Hall, Los Angeles, CA 90095-1524, USA. (yxue@geog.ucla.edu)

0148-0227/12/2012JD017692

and summer precipitation. In another study, *Fan* [2009] employed a mesoscale model, WRF, to investigate the impact of observed soil temperature. Observed soil temperatures were used to initialize the land surface model and to provide a lower boundary condition at the bottom of the model soil layer. Application of observed soil temperature increased the soil temperature compared with the original model simulation and introduced a persistent soil heating condition that was favorable to convective development and, consequently, improved the simulation of precipitation.

[4] In this study, we investigate the role and the mechanisms of SUBT on U.S. summer precipitation. A few recent studies based on observational data have demonstrated that SUBT may be a potentially useful source for improving models' seasonal prediction. *Hu and Feng* [2004a] used surface soil temperature station data over the U.S. to analyze the variations of soil enthalpy, which was calculated using an integration of soil temperature multiplied by the heat capacity through a soil column. They found that the soil enthalpy anomaly in the top 1-m soil column could persist for about 2–3 months. A persistent negative anomaly of the soil enthalpy in the northwestern United States was related to negative anomalies of the surface temperature in that region. Subsequently, the lower-troposphere temperature and related higher-atmospheric pressure anomalies in the northwestern U.S. during late spring and the early summer months, which were based on Reanalysis data, encouraged a northward position of the lower-troposphere monsoonal ridge in the western United States and, therefore, created a circulation that favored an above-average monsoon rainfall in the southwestern U. S.. However, *Hu and Feng* [2004b] also noticed that this relationship showed a peculiar on-and-off feature in the last century; i.e., the relationship was strong in some years but became weak in other years.

[5] Furthermore, other studies have also revealed a close relationship between surface temperature and snow cover in the northwestern U.S. [*Redmond and Koch*, 1991; *Karl et al.*, 1993; *Leathers and Robinson*, 1993; *Groisman et al.*, 2004]. Based on snow observations at several hundred mountain course sites in the western U.S., *Cayan* [1996] has found that in the coastal Pacific Northwest, such as in the Cascades of Oregon and Washington, anomalous snow accumulation is affected the most by fluctuations in winter and early spring precipitation anomalies. Meanwhile, the snow anomaly patterns for those regions are also strongly associated with winter surface temperature anomalies: cooler (warmer) temperatures produce positive (negative) snow water equivalent (SWE) anomalies.

[6] Several investigators, based on the data from the snow course sites and the precipitation network, have demonstrated an inverse relationship between spring snow mass in the western United States (U.S.) and subsequent summer precipitation over the southwestern U.S., associated with the North American monsoon system. Winters with high precipitation (lower spring temperature) tend to be followed by drier summers and vice versa [*Gutzler*, 2000; *Higgins and Shi*, 2000; *Lo and Clark*, 2002]. They also found that the snow–monsoon relationship was unstable over time and space. In addition, a recent modeling study [*Notaro and Zarrin*, 2011], which assigned a normal snow cover condition and a double snow depth condition over the Rocky Mountain area in a regional climate model, found that a deep Rocky Mountain snowpack tended to hinder the poleward advance of the subtropical ridge and associated monsoon rainfall in the southwest United States. A deep, extensive snowpack increases the surface albedo and provides an abundant surge of soil moisture, both of which reduce tropospheric temperatures in spring and early summer, weakening the land ocean thermal gradient and related monsoon system. This mechanism is similar to that discussed in *Carleton and Carpenter* [1990], *Gutzler* [2000], and *Hu and Feng* [2004a].

[7] All these western U.S. climate studies focus on the northwestern U.S. snow/soil temperature and southwestern U.S. monsoon precipitation relationship. Furthermore, *Hu and Feng*'s [2004a] analysis did not distinguish whether the correlations with atmospheric fields were caused by the snow condition or soil enthalpy or both since snow and soil enthalpy were highly correlated in the region. In this study, we use the nested NCEP GCM and the Eta regional climate model to identify and understand the roles of SUBT memory processes in the western U.S. in affecting North American regional climate variability at intraseasonal scales and explore an approach to improve the capability to make reliable predictions of precipitation. Furthermore, since an important climate phenomenon is the drastic decline in mountain snowpack since 1950 at about 75% of locations monitored in western North America [*Mote*, 2006], and since snow cover and soil temperature are highly correlated [*Groisman et al.*, 2004], understanding the role of SUBT in the climate system should provide useful information for climate variability and climate change studies.

2. Experimental Design

2.1. Background

[8] This section discusses a few statistics and analyses which underpin the experimental design in this study. Based on Climate Prediction Center (CPC) Merged Analysis of Precipitation (CMAP) data [*Xie and Arkin*, 1997] and Climate Anomaly Monitoring System (CAMS) surface temperature station data [*Ropelewski et al.*, 1985], we have also examine the association between winter precipitation and spring surface temperature over the western U.S. (Figure 1). Figure 1a shows the interannual variability of May surface temperature over Area TS and December–January–February (DJF) precipitation over Area P1 (see Figures 1b and 1c for the definitions of the TS and P1 areas). These two areas are selected based on the differences of precipitation and temperature between 1998, a very cold winter with relatively heavy snow, and 1992, a rather warm and dry winter, as indicated in Figure 1a. Please note that the precipitation anomaly in Figure 1a has been multiplied by minus one due to negative correlation between precipitation and temperature. The correlation between winter precipitation and spring surface temperature was -0.37 with statistical significance at the 90% level. This relationship is consistent with the studies discussed in the Introduction.

[9] Furthermore, we found that there was also a relationship between temperature in the West and precipitation in southeastern U.S. during summer. Figure 1a shows the time series of June–July–August (JJA) precipitation over the southeastern U.S. and its correlations with winter

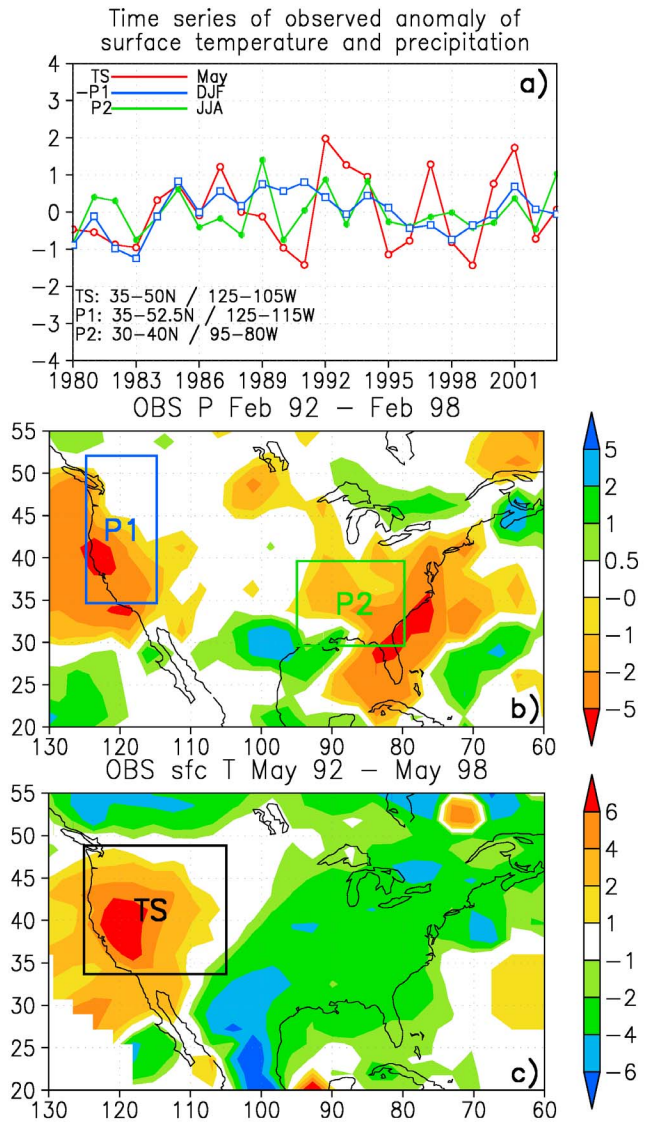

Figure 1. Observed temperature and precipitation. (a) Time series of observed anomalies of surface temperature and precipitation. (b) Observed precipitation difference between February 1992 and February 1998. (c) Observed surface air temperature difference between May 1992 and May 1998. Unit: Precipitation: mm day^{-1}, temperature: °C.

precipitation and spring temperature in the western U.S, which are −0.44 and 0.37, respectively. Those correlations are statistically significant at the 95% and 90% levels, respectively. To understand whether this relationship is physically based and more pronounced than expected from sampling variability, experiments are designed to investigate this relationship and to elucidate mechanisms that cause this correlation. The spatial anomaly distribution discussed in this section provides information for the experiments discussed in this study.

2.2. Experiment Description

[10] The regional climate Eta/Simplified Simple Biosphere (SSiB) regional climate model (RCM) with 80-km horizontal resolution [*Xue et al.*, 2001] and the NCEP Global Forecasting System (GFS) T62 coupled with the SSiB model [*Xue et al.*, 2004] were used for this study. Subsurface heat storage in SSiB is represented by two state variables: the land surface temperature (T_s) and the SUBT (T_d). A modified Force-Restore method [*Deardorff*, 1978; *Dickinson*, 1988; *Xue et al.*, 1996] is used to calculate the heat transfer between these two reservoirs.

$$C_d \frac{\partial T_d}{\partial t} = -\omega C_{gs}(T_D - T_{gs}) \quad (1)$$

where C_{gs} is the effective heat capacity of the surface soil layer and snow (J m^{-2} K^{-1}), which in the model corresponds to about 2-cm soil layer thickness; C_d is the effective heat capacity of snow-free soil, which corresponds to about 1- to 2-m soil thickness depending on the vegetation types and soil conditions [*Sellers et al.*, 1996]; and ω is the frequency of the seasonal soil temperature cycle. By comparison of the ground heat flux anomalies produced by the Force- Restore Method and a more complex model that uses a sophisticated heat transport scheme and multilayer temperature in the vertical, *Mahanama et al.* [2008] found that ground heat flux produced by the Force-Restore method did capture the first order interannual variability produced by the more complex soil model. The Eta/SSiB and NCEP GCM/SSiB's simulations of precipitation and surface temperatures have been extensively evaluated in a number of coupled model studies [e.g., *Xue et al.*, 2001, 2007, 2010] and numerous offline investigations (parts of evaluations are discussed in *Xue et al.* [2001]).

[11] In this study, the GCM and the Eta were integrated for two months from May 1–10, 1998, through June 30, 1998, with two different initial SUBT conditions over the western U.S (one from May 1998 and another from May 1992) to preliminarily explore the impact and mechanisms of the spring SUBT on the June precipitation. The case studies using RCMs with a selected year have been used to explore a number of scientific issues [e.g., *Liang et al.*, 2001; *Xue et al.*, 2007]. The year 1998 had a very cold winter and the year 1992 had a rather warm winter, as indicated in Figure 1. The performance of the Eta model for the 1998 summer simulation has been comprehensively evaluated when this summer was selected as a case study to explore the RCM downscaling issues [*Xue et al.*, 2007]. Since the surface soil temperature is normally modified by the incoming radiation and atmospheric conditions in just a couple of days, we employed a SUBT anomaly in this study. In one experiment (referred to as Case C1), the May 1998 SUBT from Reanalysis II [*Kanamitsu et al.*, 2002] was used as the initial condition, corresponding to cooler years. In another experiment (Case W1), a SUBT anomaly over the western U.S. (Figure 2a) based on Reanalysis II subsurface soil temperature in 1992 was imposed on Case C1's initial SUBT conditions, representing warm years. In this preliminary study, large subsurface temperature anomalies based on the observed surface temperature were assigned in the experiments to obtain strong response. We refer to this initial SUBT anomaly area as the Heating Area in this paper. The SUBT anomalies (Figure 2a) based on Reanalysis II were generally consistent with the CAMS surface temperature anomaly (Figure 1c). Each case in this study consisted of 10 ensemble members with different

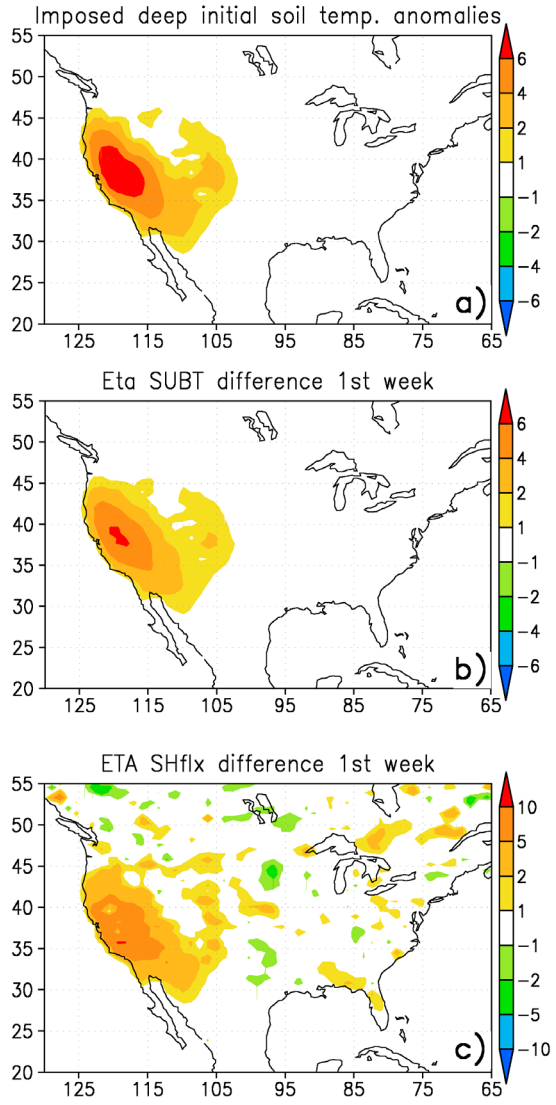

Figure 2. (a) Imposed initial subsurface soil temperature anomalies (°C). Week 1 (b) SUBT difference (K°) and (c) sensible heat flux difference between Eta Case W1 and Eta Case C1, respectively.

initial conditions from May 1–10 based on Reanalysis II. The ensemble means were taken for analyses.

[12] In the Eta/SSiB cases, the Eta domain used in this study was the Eta operational forecast domain, which includes the continental U.S. 48 states, all of Canada and Central America, and a substantial portion of the surrounding oceans [see *Xue et al.*, 2007, Figure 3]. The initial conditions and lateral boundary conditions (LBC) were obtained from the corresponding NCEP GFS/SSiB cases. For example, the initial conditions and LBC of Eta/SSiB Case W1 starting May 10 was obtained from the corresponding NCEP GFS/SSiB Case W1 that was also integrated starting from May 10. After its initial setting, the SUBT was then updated by the SSiB during the integration. The SUBT anomalies persisted during the entire integration period but became weaker as the integration continued. Figure 2b shows the average of SUBT for the 1st week. In the third week of May, the SUBT anomalies over the area initially with more than 4°C anomalies (Figure 2a) were reduced by 2° to 4°C. In June, the temperature anomaly area shown in Figure 2a kept the anomalies between 1 and 2°C (not shown).

[13] Most regional climate models' sensitivity experiments normally apply reanalysis data for both control and sensitivity runs' LBC. To test the effect of the LBC in the Eta/SSiB sensitivity experiment, we conducted another set of experiments, in which 1998 Reanalysis II data were used as the Eta/SSiB LBCs in both the control run and anomaly runs. Five ensemble members were used for this set of simulations. The experiments with control and anomalous warm SUBT are referred to as Eta/SSiB Case C2 and Eta/SSiB Case W2, respectively, in this paper. Since reanalysis data were also used for the LBC, taking different starting dates as initial conditions only produced minor differences among different ensemble members. To generate five meaningfully different initial conditions, we use the breeding method [*Toth and Kalnay*, 1997] to obtain five differently perturbed initial conditions. The breeding method constructs initial conditions by adding perturbations to a control analysis and generates a limited number of perturbations that optimally represent the span of possible analysis errors. Since the analysis cycle is like a breeding cycle, the breeding technique generates perturbations in directions where past forecast errors have grown rapidly. The breeding method has been used to generate perturbations for ensemble forecasting at the NCEP since December 1992 [*Toth and Kalnay*, 1997].

3. Impact of Subsurface Soil Temperature on Precipitation

[14] The differences of observed June precipitation between 1992 and 1998 are shown in Figure 3a. There was a strong positive rainfall anomaly over the southern U.S., from New Mexico to Florida and the nearby oceans with a northwest-southeast direction over the land. To the north, there was a negative rainfall band: a crescent-shaped negative rainfall anomaly band surrounding the Great Lakes and another relatively weak negative rainfall anomaly center located to the west of 100°W and along about 50°N. As a matter of fact, the differences between five warmest years and five coldest years between 1980 to 2003 also show this anomaly feature, i.e., the positive anomaly in southeast U.S. and negative anomalies to the north (not shown). The differences between NCEP GFS/SSiB Case W1 and Case C1 are shown in Figure 3b, and the area with rainfall difference having statistical significance above 90% (T-test value > 1.33) is enclosed with black lines. The GFS simulation only produces positive rainfall anomalies in the southeastern U.S., much smaller than the observed positive anomaly areas in Figure 3a. Meanwhile, the simulated negative rainfall anomalies to the east and west of this positive anomaly between 25°N and 30°N were inconsistent with observations. The negative rainfall anomaly to the south of the Great Lakes was not simulated and the simulated negative rainfall anomalies to the west of 100°W and along about 50°N, which were close to the imposed anomaly SUBT forcing, were consistent with observation, but with larger magnitude than observed. The spatial correlation between observed anomalies (Figure 3a) and simulated difference

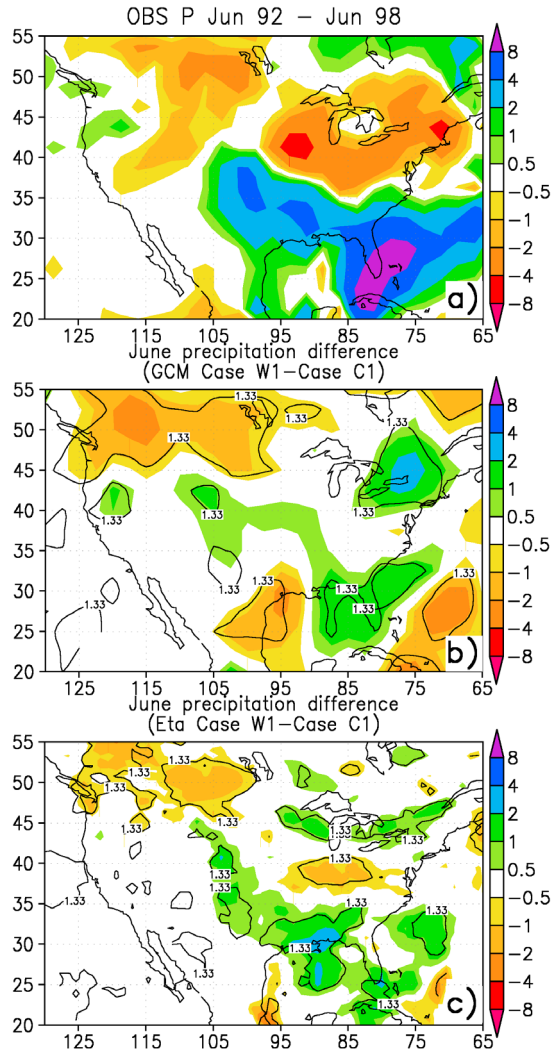

Figure 3. (a) Observed precipitation differences between June 1992 and June 1998. (b) GFS-simulated June precipitation differences between Case W1 and Case C1. (c) Eta-produced June precipitation differences between Case W1 and Case C1. Unit: Precipitation: mm day^{-1}. Contour line 1.33 indicates the 90% statistical significance level for precipitation differences.

(Figure 3b) over the domain shown in the figure was merely 0.04.

[15] Downscaling of the GFS simulation using the Eta/SSiB produces much more consistent rainfall difference patterns (Figure 3c) compared with the observed difference. The negative rainfall anomalies in the southern U.S., which appeared in the GFS simulation (Figure 3b) but were not in the observation (Figure 3a), were eliminated (Figure 3c). The negative rainfall anomaly to the south of the Great Lakes was produced by the Eta/SSiB but with much smaller extent compared with the observations. The positive rainfall anomaly in the southern U.S. with a southeast-northwest axis was well produced, especially the three highs: one near the Florida peninsula and nearby ocean, one in Louisiana, and another in eastern New Mexico and Colorado and western Texas and Kansas. However, the intensity was not as strong as in observations. Considering that this experiment only includes the effect of SUBT anomaly in the western U.S. with no snowpack difference in initial conditions and without taking other factors such as SST anomalies into account, the relatively weak response in the model simulation should be expected. Numerous studies have indicated that U.S. summer precipitation is associated with tropical and extra-tropical Pacific SST anomalies and variations of the Pacific Decadal Oscillation [e.g., *Mo and Paegle*, 2000; *Higgins and Shi*, 2000; *Nigam and Ruiz-Barradas*, 2006]. Furthermore, the extent of negative anomaly to the west of 100°W and along about 50°N was also well simulated. The peak was close to Lake Winnipeg area, consistent with observation. There are also some discrepancies between Figures 3a and 3c over the Great Lakes and Florida. The spatial correlation between the observation and the Eta simulation is 0.46, much higher than the GCMs'.

4. Impact Mechanisms

[16] To understand the mechanism of SUBT effects, the differences of vorticity and wind vectors between GFS Case W1 and GFS Case C1 as well as Eta Case W1 and Eta Case C1 at 850 hPa are shown in Figure 4. The areas with wind vector difference having statistical significance at a level above 90% (T-test value > 1.33) are enclosed with black lines. SUBT affects the surface temperature and then the surface energy balance and temperature gradient between the surface and lower atmosphere, which, in turn, affects the sensible heat flux. During the first week, the high sensible heat flux (Figure 2b) induced by warm surface conditions in the northwest U.S. in GFS Case W1 generated anomalous cyclone activity in the Heating Area (Figure 4a) and anomalous upward vertical motion (not shown), having statistical significance at a level above 90%. Outside the Heating Area, no noticeable difference was observed. Consistent with the results at 850 mb, similar anomalous cyclone features also appeared at 500 hPa but with much smaller magnitude (not shown).

[17] The disturbance propagated during the late second week and strong cyclone activity and positive vorticity started appearing in the Eastern U.S. in the third week (not shown). Figure 4b shows that during the third and fourth weeks, the perturbations as indicated by the cyclone/anticyclone and vorticity differences had established in the Eastern U.S. coastal area, showing a wave train in the GFS simulation (Figure 4b). A comprehensive analytical study based on the Complete Vorticity Equation has indicated that above the maximum heating level, an anticyclone center appears on the western side of the heating source and the cyclone center should appear on the eastern side [*Liu et al.*, 2001]. Figure 4b indeed shows these features since the maximum heating (Figure 2b) in this study was on the ground. A similar anomalous feature also appeared at 500 hPa and 200 hPa (not shown). However, the wind anomalies showed opposite change in the vertical dimension around the Heating Area; in other areas away from the Heating Area, the anomalies show barotropic vertical structure.

[18] Dynamic downscaling using the Eta model provided a much stronger response to the surface heating and produced more significant results (Figures 4d and 4e). The areas

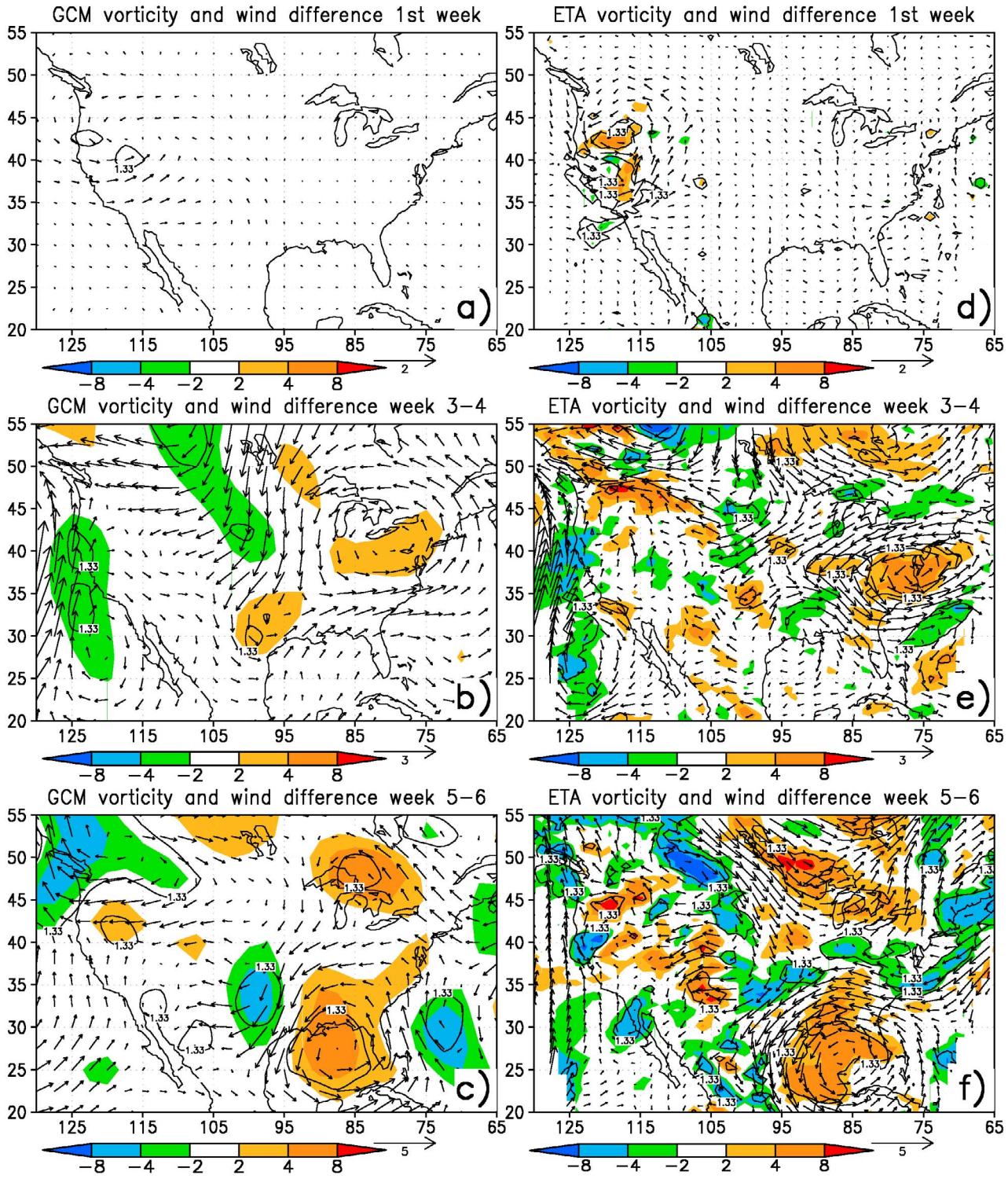

Figure 4. (a, b, and c) GFS and (d, e, and f) Eta simulated vorticity (10^{-6} s^{-1}) and wind vector (m s^{-1}) anomalies at 850 hPa. Week 1 (Figure 4a); Weeks 3–4 (Figure 4b); Weeks 5–6 (Figure 4c); Week 1 (Figure 4d); Weeks 3–4 (Figure 4e); Weeks 5–6 (Figure 4f). Contour line 1.33 indicates the 90% statistical significance level for wind vector differences.

with wind vector difference having statistical significance at a level above 90% were much larger in the Eta simulation compared with the GFS results. In the GFS simulation, over the areas with statistical significant level above 90% for wind vector difference, the vorticity difference only had a significance level above 75%. To clearly indicate improvement in simulating the impact due to dynamic downscaling in this study and emphasize the main perturbation features

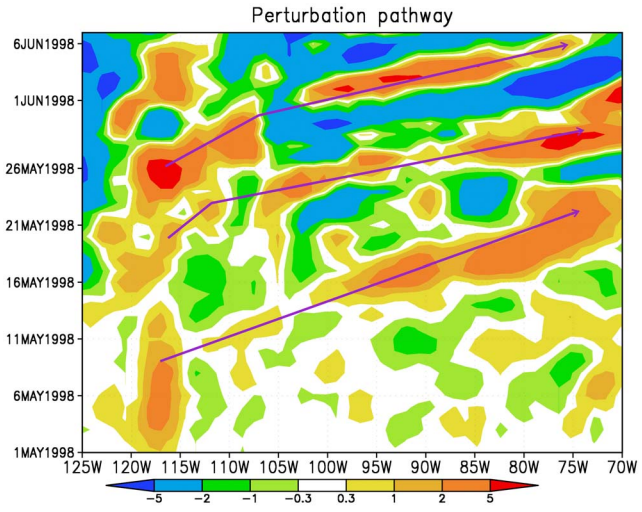

Figure 5. Perturbation pathway: temporal-zonal cross-section of vorticity anomaly (1/s) at 850 mb averaged over 35N and 50N.

caused by the SUBT anomaly, only the vorticity anomalies with statistical significance level above 90% are displayed in Figures 4d, 4e, and 4f for the Eta simulation. In the Eta case, those areas are quite consistent with the significant wind field difference areas. In the first week, significant positive vorticity anomalies in the Heating Area were shown in Figure 4d, while the GFS- produced positive anomaly was less than 0.1×10^{-5} s^{-1}. In weeks 3–4, a statistically significant cyclone and anomalous positive vorticity appeared in the eastern coastal area of the northeastern U.S. and a weaker anomalous cyclone center still can be identified on the west coast.

[19] Traveling of a cyclone can occur through propagation of planetary waves (also referred to as large-scale waves), and the Rossby wave is one of the most important. If a cyclone is thought of as the superposition of several different linear Rossby waves, the cyclone would be expected to move westward relative to the mean flow U. At midlatitudes the special identifying feature of the Rossby wave is its phase velocity (that of the wave crests) [*Holton*, 1992]. The zonal phase speed c for barotropic Rossby waves is given by

$$c = U - \frac{\beta}{k^2 + l^2} \tag{2}$$

where k and l are the zonal and meridional wave numbers and β is the parameter for the β-plane. The zonal mean flow at that pressure level can be estimated by

$$U(y,p,t) = -\frac{g}{f}\frac{\partial \overline{Z}}{\partial y} \tag{3}$$

where $\overline{Z}$ is geopotential height at the pressure level (p), f is the Coriolis parameter, and g is gravity. The zonal wave number k was about 1.8×10^{-6} m^{-1} in this case; the phase speed was about 5.4 m/s, and the mean westerly flow was about 9.4 m/s. The cyclone was propagated from (118°W, 40°N) to (80°W, 38°N) for about 10 days, consistent with the characteristic time scale required for a two-dimensional Rossby wave pattern to be set up in response to the initiation of a localized forcing in other modeling studies [*Wallace and Blackmon*, 1983]. To more clearly illustrate the perturbation pathway, Figure 5 shows the temporal-zonal cross-section of vorticity anomaly (s^{-1}) at 850 hPa averaged over 35N and 50N. The positive vorticity anomaly persists along the west coastal area due to the SUBT anomaly and propagates to the east. An anticyclone center appears on the western side of the heating source. The first disturbance propagated during the late second week and strong positive vorticity appears in the Eastern U.S. in the third week. The time used to travel perturbations to the east coast is about 7–10 days, consistent with the estimation discussed above.

[20] In weeks 3–4, the Rossby wave was nearly stationary (Figure 4), with a deep trough on the east coast as shown in the anomalous geopotential height field (Z') (Figure 6a). In weeks 5–6, the Rossby wave was still stationary in the GFS simulation (Figure 4c). The cyclone in the southern U.S. moved further eastward from Texas to the Gulf of Mexico and Florida. In the Eta downscaling, the cyclone and positive vorticity around the Gulf of Mexico was much more enhanced (Figure 4f). However, the strong negative vorticity

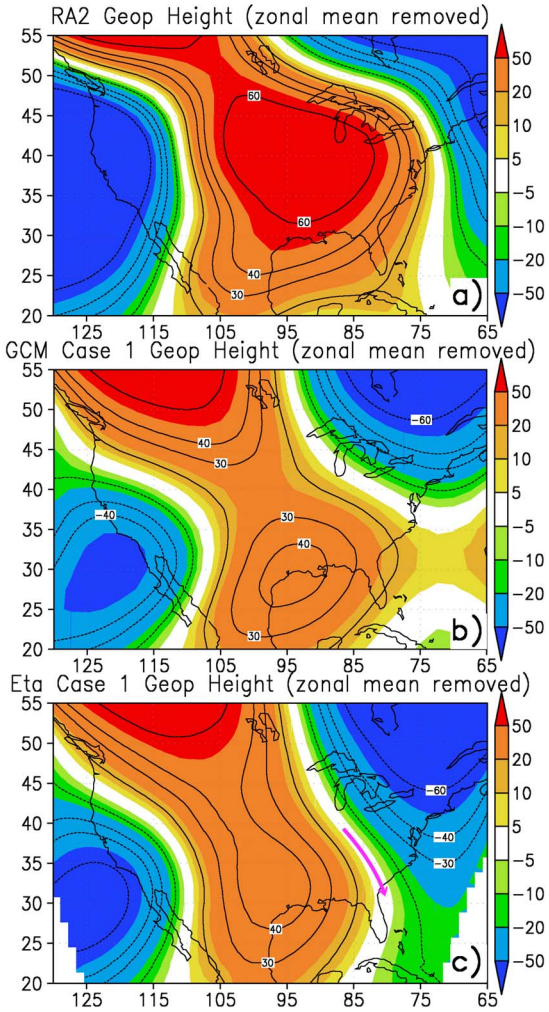

Figure 6. Geopotential height (zonal mean removed) for Weeks 3–4 at 500 hPa. (a) Reanalysis II. (b) GFS Case C1. (c) Eta Case C1. Unit: GPM.

to its west as shown in the GSF simulation (Figure 4c) did not appear; there was only a weak anticyclone (Figure 4f). This difference in the first half of June had a significant implication because the June anomalous patterns in cyclone and vorticity directly contributed to the simulated June rainfall difference shown in Figures 3b and 3c. As indicated earlier, GFS produced negative rainfall anomalies to the east and west of the southeast U.S., inconsistent with observed rainfall anomaly, while the Eta-simulated difference in rainfall in the southeastern U.S. was much closer to the observed anomalies (Figure 3).

[21] A major difference between weeks 3–4 and weeks 5–6 in the Eta simulation was the much stronger cyclone around the Gulf of Mexico and the dissipation of cyclone activity in the northeastern U.S. coastal area. The above discussion has shown that cyclones in May move together with the winds in which they are embedded. It seemed that the cyclone was steered by U during the Rossby wave propagation. Steering has been an important concept in synoptic meteorology, and steering flow indicates a basic flow that exerts a strong influence upon the direction of movement of disturbances embedded in it [*Carlson*, 1998]. Since the cyclone was moved by the total flow, it was also steered by velocity anomaly ($\mathbf{V}'$) for near zero speed of the Rossby waves ($c \cong 0$), as the Rossby wave in weeks 3–4 was nearly stationary. The anomalous meridional geostrophic wind can be estimated by

$$V'(y,p,t) = -\frac{g}{f}\frac{\partial Z'}{\partial x} \tag{4}$$

where Z' is the geopotential height anomaly. The low level cyclones move in the direction of the 500-hPa wind [*Carlson*, 1998]. To show this meridional steering effect, the zonal anomalous geopotential heights for reanalysis II, GSF Case 1, and Eta Case 1 for the late half of May in 1998 at 500 hPa are shown in Figure 6.

[22] An important relevant feature in Figure 6 is a deep trough on the east coast from the anomalous geopotential height (Z') field in Reanalysis II (Figure 6a). In this study, the Eta produced a geopotential height pattern much like Reanalysis II, while GSF's geopotential height contour line had a west-east orientation at 35°–40°N (Figure 6b), indicating limited or no steering effect for V′ there. Positive vorticity in the northeastern U.S. persisted in weeks 5–6 in the GFS simulation and contributed to the positive rainfall anomalies along the eastern coast between 40 and 45°N (Figure 3b), which is inconsistent with observed rainfall anomalies.

[23] In the Eta simulation, the southward V′ is evident (Figure 6c). We used Figure 6 to roughly estimate the value of the anomalous meridional geostrophic wind. At 38°N, Z' is about −35 m at 70°W and 0 m at 85°W. Using equation (3) leads to that of $|V'| \approx 2.9$ m s^{-1}. The cyclone moved from (77°W, 38°N) in weeks 3–4 (Figure 4e) to (87°W, 28°N) in weeks 5–6 (Figure 4f), with total traveling distance of about 1,400 km. With steering velocity ($\mathbf{V}'$) of 2.9 m s^{-1}, the total traveling time was 5.5 days (about a week) and carried the anomalous cyclone southward. The results shown in Figure 4f suggest the steering flow may play a role in the enhancement of cyclone activity in the southeastern U.S in weeks 5–6 and dissipation of the strong cyclone in northeastern U.S. in weeks 3–4. Meanwhile, the downscaling effect is also apparent for the Eta model's simulation since GFS had a cyclone over that area during weeks 5–6. Plenty of moisture availability and convective instability over the Gulf of Mexico as well as condensation heating-produced positive feedback may also contribute to the strong cyclone in weeks 5–6. The midlatitude cyclone persisted for a month in that area during all of June (not shown). The anomalous positive vorticity and cyclone in Figures 4c and 4f were very consistent with the rainfall changes shown in Figures 3b and 3c, respectively.

[24] We have checked the May 16–31 mean 500-hPa geopotential height from 1979 through 2010 in the NCEP Reanalysis II. It appears that among 32 years, 22 years had similar anomaly patterns, i.e., a low geopotential height along the North American eastern coast. Whether this climate feature contributes to the significant correlation between western coast SUBT anomaly (and snow anomaly) in the northwestern U.S. in spring and June rainfall anomaly in the southeastern U.S. (as discussed in the Introduction) needs to be investigated further.

5. LBC Impact

[25] In Eta Case W1 and Eta Case C1, the GFS Case W1 and GFS Case C1 results were used, respectively, as LBC for the Eta RCM downscaling. Since the same anomalous SUBT were used for both GFS and Eta simulations, a question would be if it is necessary to use GFS sensitivity results for downscaling rather than simply applying reanalysis data as LBC for both Eta control and sensitivity experiments as done in many RCM sensitivity studies. Although the reanalysis data are ideal for downscaling climate information from coarse resolution to high resolution, there are not many discussions on whether reanalysis is ideal for sensitivity studies. To test the effect of LBC on the results of sensitivity experiments, we conducted two additional experiments, Case C2 and Case W2, similar to Case C1 and Case W1 but with 1998 Reanalysis II data as LBCs for both experiments. Each case consists of 5 ensemble members. As discussed earlier, the breeding method [*Toth and Kalnay*, 1997] was applied to generate different initial conditions to evaluate the internal variability. This set of experiments was intended to test whether imposed anomalous forcing in the RCM alone in this study was sufficient to generate statistically significant impact regardless of the imposed LBCs. If this is the case, then discussions in the last section would be questionable because it would not be necessary to downscaling anomaly; the initial anomaly imposed in the RCM alone would be sufficient to generate proper response in the RCM simulation. In other words, the RCM itself with imposed local anomaly in the study would be able to produce a significant impact.

[26] Figures 7a and 7b show the wind vector and vorticity differences between Case W2 and Case C2 for the first week and weeks 3–4. As in Figure 4, the area with wind difference having statistical significance above 90% (T-test value > 1.33) is enclosed with black lines. In Figure 7, we show the vorticity difference with statistical significance level above 75% to emphasize the major spatial structure.

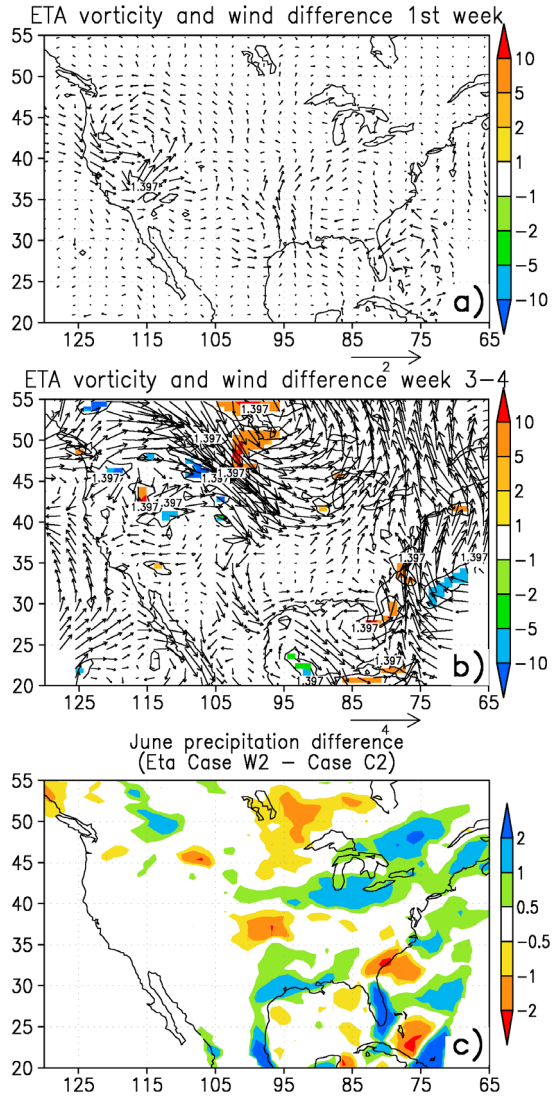

Figure 7. Eta simulated vorticity (10^{-6} s^{-1}) and wind vector (m s^{-1}) anomalies at 850 hPa for Case W1 and Case C2. (a) First week. (b) Weeks 3–4. (c) Eta-produced June precipitation difference between Case W2 and Case C2. Unit: Precipitation: mm day^{-1}.

In the first week, the anomalous cyclone was developed in the Heating Area as in Case W1 and Case C1. We also found that the perturbation traveled east in the second and third week but did not reach the East Coast, indicating that the same large scale forcing in Case W2 and Case C2 hinders the perturbation propagation as shown in Figure 7b. By weeks 5–6, there were no meaningful spatial anomaly patterns anymore (not shown). The June rainfall differences between Case W2 and Case C2 (Figure 7c) were quite consistent with wind and vorticity differences in weeks 5–6 but no statistically significant results were identified. The simulated positive rainfall anomalies along the coast of the Gulf of Mexico were also quite different from the observed difference between 1992 and 1998.

[27] The RCM is designed to keep the large scale features from the imposed LBC and produce fine resolution features [*Xue et al.*, 2007] such that the similarity and consistency in large scale features between RCM simulation and LBC are considered a successful downscaling. Because of this fundamental principle in RCM modeling, in Case W2 and Case C1, although the heating anomalies initially produced the disturbance and its movement, this effect was eventually compromised by the imposed large scale forcing and disappeared within internal noise. This experiment suggests that when the impact of anomalous local forcing is through wave propagation in a large-scale atmosphere, the RCM forced by the same LBC may have severely degraded impact due to constraints imposed by LBCs. Care must be taken regarding the LBC selection to conduct sensitivity studies using RCMs.

6. Conclusion

[28] Although the impact of SST on the climate has been extensively investigated for decades, the exploration of the SUBT's role in the climate system is generally lacking. This study explores the impact of spring SUBT anomaly due to snow anomaly in the western U.S. on North American summer precipitation, mainly the southeastern U.S., using a GCM and a RCM. The GCM was used to provide the LBCs for corresponding RCM cases. In this preliminary study, large anomalies based on the observed surface temperatures were assigned in the experiments. The idea was that if such large changes in the SUBT were unable to produce substantial variations in the simulated regional climate, further research in this direction probably would be in vain. This type of approach has been taken in many other sensitivity studies to identify the impact and mechanisms of the land processes (such as albedo and soil moisture), stimulate more scientific interest, and enhance societal support for further investigation.

[29] The Eta results with 10 ensemble members suggest that antecedent May 1st warm initial SUBT over the western U.S. contributed positive June precipitation over the southern U.S., consistent with the observed statistically significant relationship between western SUBT anomaly and southeastern U.S. summer precipitation. Meanwhile, there was less precipitation to the north of this positive rainfall area, as well as another relatively weak negative rainfall anomaly located to the west of 100°W and along about 50°N, near the Heating Area. The spatial anomaly patterns of precipitation from the Eta model were consistent with observed differences between a year with a warm spring and a year with a cold spring. The enforced temperature anomalies first induced cyclone activity in the initial SUBT anomaly area. The cyclones were then propagated eastward through Rossby waves in westerly mean flow. In addition, the steering flow produced by geopotential height gradient may contribute to the dissipation of cyclone activity in the northeastern U.S. that existed in weeks 3–4 and the enhancement of cyclones in the southeastern U.S. in weeks 5–6. Although the GCM also produced Rossby wave propagation, the results were not as significance as the Eta results. Meanwhile, the southward steering flow effect was missing due to poor simulation of the geopotential height, which caused inconsistent features in its simulated rainfall anomalies, compared to the observation. This study demonstrates that although

GFS runs with large internal variability and coarse resolutions were unable to produce adequate precipitation difference patterns, the downscaling of GFS precipitation output using Eta did yield significant results consistent with observations.

[30] The Eta results were obtained only when we used GFS outputs for the corresponding Eta runs' LBCs. When we applied the same reanalysis data for both (control and sensitivity) Eta runs' LBCs, the Rossby wave propagation was suppressed and observed precipitation anomalies were not properly produced. Because large scale circulation and low-level moisture transfer played crucial roles in proper simulations of the U.S. summer precipitation, maintaining the same LBC produced similar large-scale patterns, causing severe limitations in this sensitivity study. Downscaled regional climate is closely linked to the imposed global climate forcing. Therefore, for climate sensitivity studies using RCMs, consistent lateral boundary forcing may be crucial, especially when the impact is produced through wave transference in the atmosphere.

[31] This is the first modeling study to explore the western U.S. SUBT impact and its teleconnections with Eastern U.S. precipitation. The results suggest that SUBT may be able to provide an extended element of memory, which would enhance predictability. However, there are many issues which require more investigations. Studies have found that the snow/enthalpy–monsoon relationship is unstable over time and space and it has been speculated that the SST's effect may complicate this relationship [*Gutzler*, 2000; *Lo and Clark*, 2002; *Hu and Feng*, 2004a]. The mechanism in this study involves the perturbation propagation and synoptic processes. *Wallace and Blackmon* [1983] pointed out that due to chaos in individual realizations the spatial pattern of perturbation may not be very robust. More case studies are needed to further explore its effect and mechanisms. Moreover, since this study only considered the SUBT forcing, the simulated precipitation anomaly was smaller than observed. The statistics presented in the introduction show a positive correlation between May temperature and summer precipitation. This study only finds the May temperature's impact on June precipitation. Its effect on July precipitation is unclear. It is necessary to apply modeling studies and data analyses to understand the role of SUBT under different climate conditions, as well as its interaction with SST and snow in the climate system with more case investigations. Further investigation with full snow anomaly and SST forcings are warrant. Furthermore, this study discusses the impact of the SUBT anomaly over mountain regions. We also conducted an experiment with the SUBT anomaly over the entire domain as shown in Figure 1c. The results were very similar to that from Case W1 (not shown). The relative role/impact of SUBT at high and low elevations needs further investigation. More soil temperature data available from ground measurements and satellite observations and more sophisticated multilayer soil models [e.g., *Li et al.*, 2010] should help us to have more extensive research in this field.

[32] **Acknowledgments.** This research was supported by NOAA grants NA05OAR4310010 and NA07OAR4310226 and by U.S. National Science Foundation grant ATM-0751030. The NCAR super computer was used for the computation. The authors sincerely thank Lan Yi for her early work on this paper and Y. Zhu of NCEP for his help in applying the Breeding Method for the ensemble simulation. We also appreciate David Neelin of UCLA's very constructive and helpful discussions.

References

Carleton, A. M., and D. A. Carpenter (1990), Mechanisms of interannual variability of the southwest United States summer rainfall maximum, *J. Clim.*, *3*, 999–1015, doi:10.1175/1520-0442(1990)003<0999:MOIVOT>2.0.CO;2.

Carlson, T. N. (1998), *Midlatitude Weather Systems*, 507 pp., Am. Meteorol. Soc., Boston, Mass.

Cayan, D. R. (1996), Interannual climate variability and snowpack in the western United States, *J. Clim.*, *9*, 928–948, doi:10.1175/1520-0442(1996)009<0928:ICVASI>2.0.CO;2.

Deardorff, J. W. (1978), Efficient prediction of ground surface temperature and moisture, with inclusion of a layer of vegetation, *J. Geophys. Res.*, *83*, 1889–1903, doi:10.1029/JC083iC04p01889.

Dickinson, R. E. (1988), The force-restore model for surface temperature and its generalization, *J. Clim.*, *1*, 1086–1097, doi:10.1175/1520-0442(1988)001<1086:TFMFST>2.0.CO;2.

Dirmeyer, P. A., C. A. Schlosser, and K. L. Brubaker (2009), Precipitation, recycling, and land memory: An integrated analysis, *J. Hydrometeorol.*, *10*, 278–288, doi:10.1175/2008JHM1016.1.

Fan, X. (2009), Impacts of soil heating condition on precipitation simulations in the Weather Research and Forecasting model, *Mon. Weather Rev.*, *137*, 2263–2285, doi:10.1175/2009MWR2684.1.

Groisman, P. Y., R. W. Knight, T. R. Karl, D. R. Easterling, B. Sun, and J. H. Lawrimore (2004), Contemporary changes of the hydrological cycle over the contiguous United States: Trends derived from in situ observations, *J. Hydrometeorol.*, *5*, 64–85, doi:10.1175/1525-7541(2004)005<0064:CCOTHC>2.0.CO;2.

Gutzler, D. S. (2000), Covariability of Spring snowpack and summer rainfall across the southwest United States, *J. Clim.*, *13*, 4018–4027, doi:10.1175/1520-0442(2000)013<4018:COSSAS>2.0.CO;2.

Higgins, R. W., and W. Shi (2000), Dominant factors responsible for interannual variability of the summer monsoon in the southwestern United States, *J. Clim.*, *13*, 759–776, doi:10.1175/1520-0442(2000)013<0759:DFRFIV>2.0.CO;2.

Holton, J. R. (1992), Rossby waves, in *An Introduction to Dynamic Meteorology*, 3rd ed., pp. 216–221, Academic, San Diego, Calif.

Hu, Q., and S. Feng (2004a), A role of the soil enthalpy in land memory, *J. Clim.*, *17*, 3633–3643, doi:10.1175/1520-0442(2004)017<3633:AROTSE>2.0.CO;2.

Hu, Q., and S. Feng (2004b), Why has the land memory changed?, *J. Clim.*, *17*, 3236–3243, doi:10.1175/1520-0442(2004)017<3236:WHTLMC>2.0.CO;2.

Kanamitsu, M., W. Ebisuzaki, J. Woollen, S.-K. Yang, J. J. Hnilo, M. Fiorino, and G. L. Potter (2002), NCEP–DOE AMIP-II Reanalysis (R-2), *Bull. Am. Meteorol. Soc.*, *83*, 1631–1643, doi:10.1175/BAMS-83-11-1631.

Karl, T. R., P. V. Groisman, R. W. Knight, and R. R. Heim (1993), Recent variations of snow cover and snowfall in North America and their relation to precipitation and temperature variations, *J. Clim.*, *6*, 1327–1344, doi:10.1175/1520-0442(1993)006<1327:RVOSCA>2.0.CO;2.

Leathers, D. J., and D. A. Robinson (1993), The association between extremes in North American snow cover and United States temperature, *J. Clim.*, *6*, 1345–1355, doi:10.1175/1520-0442(1993)006<1345:TABEIN>2.0.CO;2.

Li, Q., S. Sun, and Y. Xue (2010), Analyses and development of a hierarchy of frozen soil models for cold region study, *J. Geophys. Res.*, *115*, D03107, doi:10.1029/2009JD012530.

Liang, X.-Z., K. E. Kunkel, and A. N. Samel (2001), Development of a regional climate model for U.S. Midwest applications. Part I: Sensitivity to buffer zone treatment, *J. Clim.*, *14*, 4363–4378, doi:10.1175/1520-0442(2001)014<4363:DOARCM>2.0.CO;2.

Liu, Y. M., G. X. Wu, H. Liu, and P. Liu (2001), Condensation heating of Asian summer monsoon and the subtropical anticyclone in the Eastern Hemisphere, *Clim. Dyn.*, *17*, 327–338, doi:10.1007/s003820000117.

Lo, F., and M. P. Clark (2002), Relationships between spring snow mass and summer precipitation in the southwestern United States associated with the North American monsoon system, *J. Clim.*, *15*, 1378–1385, doi:10.1175/1520-0442(2002)015<1378:RBSSMA>2.0.CO;2.

Mahanama, S. P. P., R. D. Koster, R. H. Reichle, and M. J. Suarez (2008), Impact of subsurface temperature variability on surface air temperature variability: An AGCM study, *J. Hydrometeorol.*, *9*, 804–815, doi:10.1175/2008JHM949.1.

Mo, K. C., and J. N. Paegle (2000), Influence of sea surface temperature anomalies on the precipitation regimes over the southwest United States, *J. Clim.*, *13*, 3588–3598, doi:10.1175/1520-0442(2000)013<3588:IOSSTA>2.0.CO;2.

Mote, P. W. (2006), Climate-driven variability and trends in mountain snowpack in western North America, *J. Clim.*, *19*, 6209–6220, doi:10.1175/JCLI3971.1.

Nigam, S., and A. Ruiz-Barradas (2006), Seasonal hydroclimate variability over North America in global and regional reanalyses and AMIP simulations: Varied representation, *J. Clim.*, *19*, 815–837, doi:10.1175/JCLI3635.1.

Notaro, M., and A. Zarrin (2011), Sensitivity of the North American monsoon to antecedent Rocky Mountain snowpack, *Geophys. Res. Lett.*, *38*, L17403, doi:10.1029/2011GL048803.

Redmond, H. T., and R. W. Koch (1991), Surface climate and streamflow variability in the western United States and their relationship to large scale circulation indices. *Water Resour. Res.*, *27*, 2381–2399, doi:10.1029/91WR00690.

Ropelewski, C. F., J. E. Jonowiak, and M. E. Halper (1985), The analysis and display of real time surface climate data, *Mon. Weather Rev.*, *113*, 1101–1106, doi:10.1175/1520-0493(1985)113<1101:TAADOR>2.0.CO;2.

Sellers, P. J., D. A. Randall, G. J. Collatz, J. A. Berry, C. B. Field, D. A. Dazlich, C. Zhang, G. D. Collelo, and L. Bounoua (1996), A. revised land surface parameterization (SiB2) for atmospheric GCMs. 1. Model formulation, *J. Clim.*, *9*, 676–705, doi:10.1175/1520-0442(1996)009<0676:ARLSPF>2.0.CO;2.

Toth, Z., and E. Kalnay (1997), Ensemble forecasting at NCEP and the breeding method, *Mon. Weather Rev.*, *125*, 3297–3319, doi:10.1175/1520-0493(1997)125<3297:EFANAT>2.0.CO;2.

Wallace, J. M., and M. L. Blackmon (1983), Observations of low-frequency atmospheric variability, in *Large Scale Dynamical Processes in the Atmosphere*, edited by B. J. Hoskins and R. P. Pearce, pp. 55–94, Academic, San Diego, Calif.

Xie, P., and P. A. Arkin (1997), Global precipitation: A 17-year monthly analysis based on gauge observations, satellite estimates, and numerical model outputs, *Bull. Am. Meteorol. Soc.*, *78*, 2539–2558, doi:10.1175/1520-0477(1997)078<2539:GPAYMA>2.0.CO;2.

Xue, Y., F. J. Zeng, and C. A. Schlosser (1996), SSiB and its sensitivity to soil properties—A case study using HAPEX-Mobilhy data, *Global Planet. Change*, *13*, 183–194, doi:10.1016/0921-8181(95)00045-3.

Xue, Y., F. J. Zeng, K. Mitchell, Z. Janjic, and E. Rogers (2001), The impact of land surface processes on simulations of the U.S. hydrological cycle: A case study of the 1993 flood using the SSiB land surface model in the NCEP Eta Regional Model, *Mon. Weather Rev.*, *129*, 2833–2860, doi:10.1175/1520-0493(2001)129<2833:TIOLSP>2.0.CO;2.

Xue, Y., H.-M. H. Juang, W.-P. Li, S. Prince, R. DeFries, Y. Jiao, and R. Vasic (2004), Role of land surface processes in monsoon development: East Asia and West Africa, *J. Geophys. Res.*, *109*, D03105, doi:10.1029/2003JD003556.

Xue, Y., R. Vasic, Z. Janjic, F. Mesinger, and K. E. Mitchell (2007), Assessment of dynamic downscaling of the continental U.S. regional climate using the Eta/SSiB Regional Climate Model, *J. Clim.*, *20*, 4172–4193, doi:10.1175/JCLI4239.1.

Xue, Y., F. De Sales, R. Vasic, C. R. Mechooso, S. D. Prince, and A. Arakawa (2010), Global and temporal characteristics of seasonal climate/vegetation biophysical process (VBP) interactions, *J. Clim.*, *23*, 1411–1433, doi:10.1175/2009JCLI3054.1.

Zhou, L., R. K. Kaufmann, Y. Tian, R. B. Myneni, and C. J. Tucker (2003), Relation between interannual variations in satellite measures of northern forest greenness and climate between 1982 and 1999, *J. Geophys. Res.*, *108*(D1), 4004, doi:10.1029/2002JD002510.